

An Intuitive Semiclassical Picture of Proton Structure at Small x

GÖSTA GUSTAFSON

Dept. of Theoretical Physics, Lund University
Sölvegatan 14A, S-22362 Lund, Sweden

Dedicated to Jan Kwieciński on his 65th birthday

A semiclassical description of structure functions in DIS at small x is presented. It gives an intuitive picture of the transition from the Double Leading Log approximation at large Q^2 , to the powerlike dependence on x in the BFKL region at limited Q^2 . Formal derivations from perturbative QCD, *e.g.* in the BFKL or the CCFM formalisms, are technically complicated, and therefore such an intuitive picture may be valuable and possibly helpful in the work towards a better understanding of DIS, and of the strong interaction in general.

PACS numbers: 12.38-t, 13.60.Hb

1. Introduction

Experiments which study deep inelastic ep scattering (DIS) have given decisive information about the basic structure of matter. Results from the linear accelerator at SLAC [1] gave the first evidence for a pointlike substructure in the proton. At the higher energies available at the HERA collider at DESY it has been possible to penetrate still deeper into the proton. DIS has the advantage over *e.g.* e^+e^- -annihilation and hadronic collisions, that there are two different scales, the total hadronic energy W and the photon virtuality Q^2 , which can be varied independently. This offers a unique possibility to study the interplay between the perturbative and non-perturbative regimes in strong interaction.

A remarkable result at HERA is the observation that for a fixed limited value of Q^2 , the γ^*p cross section grows very rapidly for large W or small $x_{Bj} \equiv Q^2/(W^2 + Q^2)$, approximately proportional to $x_{Bj}^{-\lambda} \sim (W^2)^\lambda$ with $\lambda \sim 0.3$. Such a strong increase, which is significantly stronger than the corresponding growth of the pp cross section at similar energies, was predicted

by the BFKL [2] evolution formalism, based on the exchange of perturbative gluon chains. Indeed, in leading logarithmic order the BFKL equation predicts an even stronger increase than what is experimentally observed.

The significance of the BFKL result is somewhat reduced by the facts that first the next to leading order correction is very large, secondly the introduction of a running coupling would favour chains close to the non-perturbative region, which makes the result sensitive to a necessary soft cutoff. Both of these effects make the perturbative expansion less reliable. Although the experimental results do indicate that some hard perturbative mechanism is at work, it has also been possible to fit the data without the BFKL mechanism, provided the soft nonperturbative input gluon distribution grows sufficiently rapidly for small x_{Bj} . Measurements of the total cross section, described by the structure function F_2 , cannot separate between the different mechanisms. Further experimental studies of the properties of the final states are needed, in parallel with theoretical work to distinguish between different possibilities.

The derivation of the BFKL equation, and also of the CCFM equation [3] which interpolates between the finite- Q^2 -BFKL and the large- Q^2 regimes, are technically quite complicated. A semiclassical description, which can give an intuitive picture of the results, may therefore be valuable and possibly helpful in the work towards a better understanding of DIS, and of the strong interaction in general. An attempt for such a picture will be presented in the sections 2 - 5 below.

The Linked Dipole Chain model (LDC) [4] is a reformulation and generalization of the CCFM model. The formalism in the LDC model has great similarities with the description in the semiclassical model presented here, and thus it offers a quantitative motivation for the qualitative results in our intuitive picture. A very brief description of the LDC model is presented in section 6, including also a discussion of possible applications to hadronic collisions.

In this article I want to emphasize the similarities between QCD and QED, and have therefore repeated wellknown results from electrodynamics. Large parts may therefore appear rather trivial to many readers, who consequently may omit these sections.

2. Bremsstrahlung in Electrodynamics

2.1. Photon emission

Let us study a charged particle with momentum p_1 , which emits a photon with momentum q , and after recoil has obtained momentum $p_2 = p_1 - q$, see fig. 1. The interaction between a charged scalar particle and the

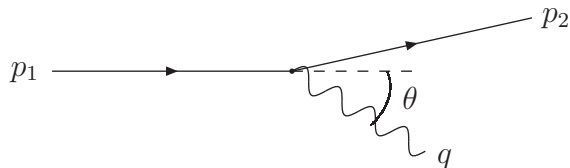


Fig. 1. A particle with momentum p_1 emits a photon with momentum q , and obtains after recoil momentum $p_2 = p_1 - q$.

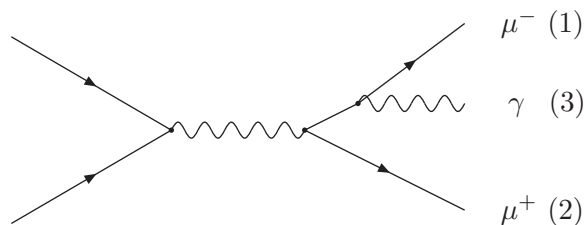


Fig. 2. e^+e^- -annihilation into a $\mu^+\mu^-$ pair and a photon.

electromagnetic field is described by the interaction term

$$\sim e j_\mu A_\mu \sim e(p_1 + p_2)_\mu \epsilon_\mu. \quad (1)$$

This contribution depends only on the trajectory of the charged particle, and corresponds to what is called the “eikonal current”. The resulting emission spectrum can be presented in different equivalent forms

$$dn \sim \alpha \frac{d\theta^2}{\theta^2} \frac{dq_0}{q_0} \sim \alpha \frac{dq_\perp^2}{q_\perp^2} \frac{dz}{z} \sim \alpha \frac{dq_\perp^2}{q_\perp^2} dy, \quad (2)$$

where $z = q_0/p_{1,0}$ is the fraction of the parent energy given to the photon, and $y = \frac{1}{2} \ln \frac{q_0 + q_L}{q_0 - q_L}$.

As an example we look at e^+e^- -annihilation into a $\mu^+\mu^-$ pair and a photon, see fig. 2. If the scaled energies of the μ^- , the μ^+ , and the photon are denoted x_1 , x_2 , and x_3 respectively, the cross section is given by

$$dn \sim \alpha \frac{dx_1 dx_2}{(1-x_1)(1-x_2)} (x_1^2 + x_2^2). \quad (3)$$

With a suitable definition of a longitudinal direction we have

$$q_\perp^2 = s(1-x_1)(1-x_2), \quad y = \frac{1}{2} \ln \left(\frac{1-x_1}{1-x_2} \right). \quad (4)$$

With this definition the factor $dx_1 dx_3 / (1 - x_1)(1 - x_3)$ in eq. (3) is identical to the expression in eq. (2), $(dq_{\perp}^2 / q_{\perp}^2) dy$. The last factor in eq. (3) is a correction factor due to the muon spin.

For collinear emission $q_{\perp} \rightarrow 0$. The squared propagator gives a factor $\sim 1/q_{\perp}^4$, but for such emissions we have $(\mathbf{p}_1 + \mathbf{p}_2) // \mathbf{q} \perp \epsilon$, which implies a suppression such that the net result is proportional to the factor $dq_{\perp}^2 / q_{\perp}^2$ in eq. (2). Thus we note that the vector nature of the photon is essential.

2.2. Ordered cascades

Sudakov form factors

The total emission probability in eq. (3) diverges, which thus gives an infinite cross section. To order α this infinity is compensated by virtual corrections to the probability for no emission, which is a negative contribution. Thus in leading order a cutoff is needed in q_{\perp} or in invariant masses $M_{\mu^+, \gamma}$ and M_{γ, μ^-} . With such a cutoff the cross sections for zero and one emission are both positive, and their sum, the first order result for the total cross section, is approximately the same as the zero's order expression. This result can be generalized to higher orders. In higher orders the probability to emit an extra photon is also compensated by a reduced probability for no emission, in such a way that the total cross section is (approximately) unaffected. Thus the annihilation process can be separated into two independent phases, the initial production of the $\mu^+ \mu^-$ pair, and the subsequent photon bremsstrahlung.

Soft emissions, for which the recoils can be neglected, are also fully uncorrelated, and the probability to emit a fixed number of photons in a given phase space region is given by a Poissonian distribution. This implies that the probability for no photon emission in a certain excluded region exponentiates, and is proportional to the ‘‘Sudakov form factor’’

$$S = \exp\left(- \int_{excl. \ region} dn\right). \quad (5)$$

This result is quite general. For processes in which an emission does not change the total reaction probability, the emission probability is normally associated with such a Sudakov form factor. We will in the following see several examples of this.

Formation time

Assume that the charged particle moves along a curved and twisted trajectory. The emission probability is proportional to

$$\left| \int j(x) e^{iqx} \right|^2. \quad (6)$$

From this expression we see that only short wavelengths can be sensitive to small deviations in the trajectory on a small timescale. For long wavelengths the integral gives the average over a larger region in space and time. This averaging implies that it takes a finite time to determine that a photon has been emitted, which can be formulated in terms of a (Landau-Pomeranchuk) formation time

$$\tau \sim 1/q_{\perp}. \quad (7)$$

Ordered emissions

The result in eq. (7) implies that in *e.g.* an e^+e^- -annihilation event the photons with large q_{\perp} are emitted rapidly, directly after the annihilation, whereas those with smaller q_{\perp} are emitted afterwards over an extended time period. When many photons are emitted, the ordering in q_{\perp} also corresponds to an ordering in time.

Looking for the first emission in time means looking for the emission of the photon with largest q_{\perp} . The probability that no photon is emitted with transverse momentum larger than q_{\perp} is determined by a Sudakov form factor. Thus the probability for emitting a photon with transverse momentum q_{\perp} as the first emission is given by

$$dn \sim \alpha \frac{dx_1 dx_2}{(1-x_1)(1-x_2)} (x_1^2 + x_2^2) \cdot S(q_{\perp}), \quad (8)$$

where the integral in $S(q_{\perp})$ extends over all transverse momenta larger than q_{\perp} :

$$S(q_{\perp}) = \exp\left(-\int_{q'_{\perp} > q_{\perp}} dn\right). \quad (9)$$

Similarly, if first a photon with transverse momentum $q_{\perp,1}$ is emitted, a second emission of a softer photon with transverse momentum $q_{\perp,2}$ is associated with the form factor $S(q_{\perp,1}, q_{\perp,2})$, defined by

$$S(q_{\perp,1}, q_{\perp,2}) = \exp\left(-\int_{q_{\perp,2}}^{q_{\perp,1}} dq_{\perp} \frac{dn}{dq_{\perp}}\right). \quad (10)$$

This process can be repeated to give a q_{\perp} -ordered cascade of emitted photons.

Spacelike cascades

In spacelike cascades we have bremsstrahlung both as initial and as final state radiation, as indicated in fig. 3. Final state radiation is very similar to the emission in e^+e^- -annihilation discussed above. The ordering due to formation time implies that also the initial radiation cascade is q_{\perp} -ordered:

$$q_{\perp,1}^2 < q_{\perp,2}^2 < \dots < q_{\perp,n}^2 < Q^2 \quad (11)$$

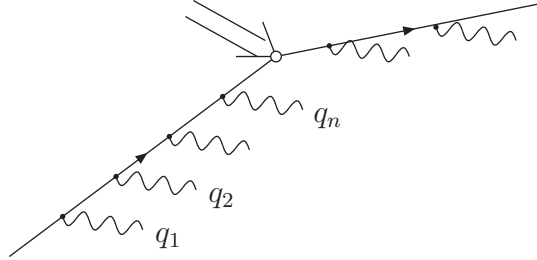


Fig. 3. A spacelike photon cascade.

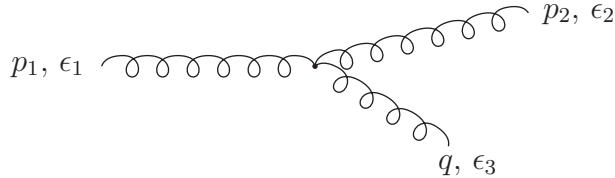


Fig. 4. Triple gluon vertex.

As mentioned earlier, neglecting recoils all photon emissions are uncorrelated, and therefore the ordering between them is not relevant. The ordering is only important when the recoils cannot be neglected, and therefore the current is modified for the subsequent emissions. However, as we will discuss more in the following, the ordering is very essential in QCD, where the emitted radiation is not neutral, but carries colour charge. This implies that an emitted gluon changes radically the current, which determines later (*i.e.* softer) radiation. Therefore the order of the emissions becomes important, and is an essential feature of the evolution processes.

We also note that the separation between initial and final state radiation in fig. 3 is gauge dependent. This separation is not determined by nature, but depends on the formalism used.

3. Bremsstrahlung in QCD, e^+e^- -annihilation

3.1. Gluon emission

In QCD the gluons carry colour charge, and therefore radiate, or split into two gluons. The dominant interaction is the triple-gluon coupling (for notation *cf.* fig. 4; ϵ_3 denotes the polarization vector for the “emitted” gluon

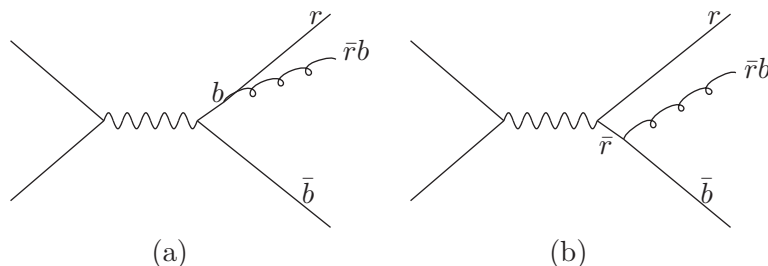


Fig. 5. A quark and an antiquark emit gluons coherently by diagrams (a) and (b). In the angular region between the quark and the gluon the red and the antired charges radiate softer gluons approximately independently, forming a $r\bar{r}$ colour dipole. At larger angles the emission from the red and the antired interfere destructively, and the quark-gluon system radiates as a single blue charge. Thus in this region the emission corresponds to a $b\bar{b}$ dipole.

with momentum q):

$$g \{ [(p_1 + p_2)\epsilon_3] (\epsilon_1\epsilon_2) - [(q + p_1)\epsilon_2] (\epsilon_3\epsilon_1) - [(p_2 - q)\epsilon_1] (\epsilon_2\epsilon_3) \} \quad (12)$$

The first term is an eikonal contribution similar to the bremsstrahlung from a quark or the electromagnetic radiation from an electron in eq. (2). The factor $\epsilon_1\epsilon_2$ implies that the recoiling parent keeps its polarization, and it gives an emission density proportional to

$$\alpha_s \frac{dq_{\perp}^2}{q_{\perp}^2} dy. \quad (13)$$

This term dominates for soft emissions. The second and third terms in eq. (12) correspond to non-eikonal currents, in which the polarization vector for the emitted gluon, ϵ_3 , is multiplied by the polarization vector for the parent gluon, either before or after the recoil.

3.2. Colour coherence

Study as an example the reaction in fig. 5a, where a blue-antiblue quark-antiquark pair is produced, and the blue quark emits a blue-antired gluon and becomes red. An identical final state can be obtained from the diagram in fig. 5b, where the gluon is emitted from an initially red antiquark, which becomes blue. The two diagrams interfere, and it is not possible to tell who is the parent to the emitted gluon. It therefore makes sense to regard the quark and the antiquark as a colour dipole, which emits gluons coherently.

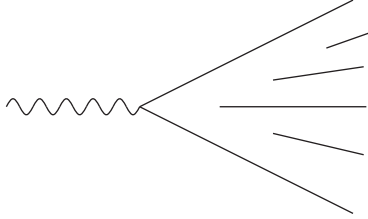


Fig. 6. A colour dipole cascade.

The emission probability is given by the corresponding expression for photon emission in eq. (3), with α replaced by α_s .

In the region between the quark and the gluon, the separation of red and antired charges will give radiation of softer gluons. However, in directions further away from these particles the emission from red and antired interferes destructively. Thus in these directions the emission corresponds to the blue and antiblue charges of the initial $q\bar{q}$ pair, i.e. the emission from a $b\bar{b}$ colour dipole. This interference effect is generally called angular ordering [5]. In the restframe of the quark and gluon, the emission of softer gluons corresponds just to a $r\bar{r}$ dipole. Thus the emission of softer gluons corresponds to two *independent* colour dipoles.

3.3. Gluon cascades

It is possible to describe a parton state in two equivalent (dual) ways [6], either in terms of momenta, q_i , and spins, s_i , for the gluons, or in terms of momenta, p_i , and directions, d_i , for the dipoles. Thus gluon emission can be described as a process in which one dipole is split into two dipoles, which are split into four, etc., as shown in fig. 6. This formulation is used in the *Dipole Cascade Model* [6, 7]. It is the basis for the ARIADNE MC [8], which has been very successfully applied to e^+e^- annihilation data, *cf. e.g.* ref. [9].

The dipole formalism is also convenient for analytic studies of the properties of QCD cascades, and we also note that the resulting chain of colour dipoles gives a very natural connection to the Lund String Fragmentation model [10].

4. DIS, DGLAP evolution

4.1. Notations

The density of quarks and gluons within the proton is described by “parton distribution functions” $f_q(x)$ and $f_g(x)$, where x is the fraction of the proton momentum carried by the parton. We will use capital letters to denote the densities in the variable $\ln 1/x$, and for simplicity we will write $F(x)$ and $G(x)$ to denote $x \cdot f_q(x)$ and $x \cdot f_g(x)$ respectively.

The electron-proton cross section is expressed in terms of structure functions F_1 and F_2 . In the parton model these functions are related to each other, and to the quark density. The exchanged photon is absorbed by a quark, which after the absorption stays on the mass shell. If q_γ and p_p denote the momenta of the photon and the proton, respectively, energy-momentum conservation is implemented by a delta-function $\delta(x - Q^2/2p_p \cdot q_\gamma)$, where $Q^2 = -q_\gamma^2$, and the ep scattering cross section can (neglecting less important kinematic factors) be written

$$\frac{d^2\sigma_{ep}}{dQ^2 d\ln 1/x} \sim \frac{\alpha^2}{Q^4} F_2(x) = \frac{\alpha^2}{Q^4} \sum_q e_q^2 x f_q(x), \quad (14)$$

where $x = x_{Bj} \equiv Q^2/2p_p \cdot q_\gamma$, the sum runs over quark species q , and e_q is the corresponding quark electric charge (in units of the elementary charge). The quantity $\frac{\alpha}{Q^2} F_2$ can also be interpreted as the total γ^*p cross section.

In the distribution functions $F(x)$ and $G(x)$ the parton densities are integrated over transverse momenta. In the following we will also discuss “non-integrated” parton distributions, which depend also on k_\perp , and which we will denote by curly letters, $\mathcal{F}(x, k_\perp^2)$ and $\mathcal{G}(x, k_\perp^2)$ for the quark and gluon densities respectively.

4.2. Ordered ladders

In the parton model the structure function F_2 and the parton distributions are functions of x only, but in QCD they also receive a dependence on Q^2 . Assume that a quark with momentum $p_0 = x_0 p$ emits a gluon with momentum $(1-z)p_0$ before interacting with the photon, as shown in fig. 7. This implies that $x = Q^2/2pq_\gamma = zx_0$. The contribution to the cross section from the eikonal current is then determined by the emission probability

$$Prob. \sim \frac{4\alpha_s}{3\pi} \frac{dz}{1-z} \frac{dq_\perp^2}{q_\perp^2} \delta(x - zx_0). \quad (15)$$

When many gluons are emitted as in fig. 8a we again obtain an ordered emission determined by the formation times:

$$q_{\perp 1}^2 < q_{\perp 2}^2 < \dots < q_{\perp n}^2 < Q^2 \quad (16)$$

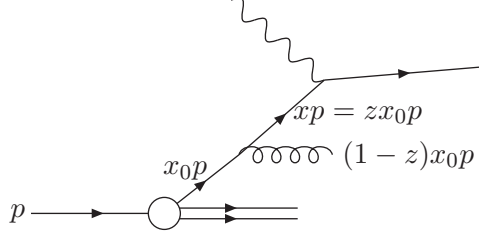


Fig. 7. A quark with momentum $p_0 = x_0 p$ emits a gluon with momentum $(1-z)p_0$ before interacting with the photon.

Thus the contribution to the structure function F from a chain with n links is given by a product of n factors

$$\frac{4\alpha_s}{3\pi} \frac{dz_i}{1-z_i} \frac{dq_{\perp,i}^2}{q_{\perp,i}^2}, \quad (17)$$

where $x = (\prod^n z_i)x_0$, and the transverse momenta satisfy the ordering condition in eq. (16).

Although many gluons are emitted in the process in fig. 8a, there is still only *one* quark, which can be hit by the photon. When Q^2 is large, the many gluons, which can be emitted before the γq interaction, imply a reduced probability to collide *without* gluon emission. The factor in eq. (17), which determines the probability to emit a gluon, must then be multiplied by a *Sudakov form factor*, S , which describes the probability that no emission has occurred between $q_{\perp,i-1}$ and $q_{\perp,i}$. Thus we have to make the following replacement in eq. (17):

$$\frac{1}{1-z_i} \frac{dq_{\perp,i}^2}{q_{\perp,i}^2} \rightarrow \frac{\theta(1-\epsilon-z_i)}{1-z_i} \frac{dq_{\perp,i}^2}{q_{\perp,i}^2} S(q_{\perp,i}^2, q_{\perp,i-1}^2) \quad (18)$$

where

$$S(q_{\perp,i}^2, q_{\perp,i-1}^2) = \exp \left[- \int_{q_{\perp,i-1}^2}^{q_{\perp,i}^2} \frac{4\alpha_s}{3\pi} \frac{dq_{\perp}^2}{q_{\perp}^2} \int_0^{1-\epsilon} \frac{dz}{1-z} \right] \quad (19)$$

We have here introduced a cutoff ϵ , which in a MC must be kept different from zero, since $\epsilon \rightarrow 0$ implies that $S \rightarrow 0$. A small ϵ gives a more accurate result, but also a slower program.

4.3. DGLAP evolution for large x

Summarizing the results in the previous subsection, and summing over the number of links, n , in the chain, we find the following expression for the

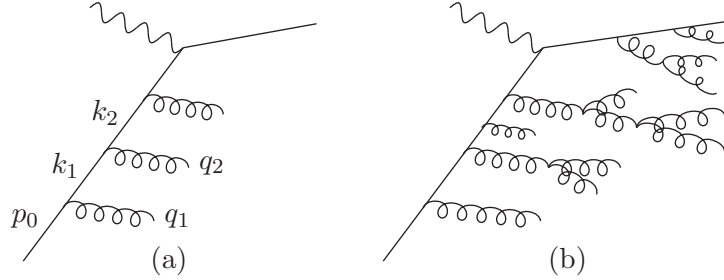


Fig. 8. (a) A chain formed by initial state radiation. (b) To describe properties of exclusive final states final state radiation has to be added. Note that a soft final state gluon also can be emitted from a virtual link, if the recoil is small. Such emissions, like the one emitted from the link k_2 in this figure, will be further discussed in section 5.5.

structure function:

$$F \sim \sum_n \prod_i^n \left\{ \int \frac{4\alpha_s}{3\pi} \frac{dz_i}{1-z_i} \frac{dq_{\perp,i}^2}{q_{\perp,i}^2} S(q_{\perp,i}^2, q_{\perp,i-1}^2) \theta(q_{\perp,i} - q_{\perp,i-1}) \right\} \times \\ \times \delta(x - \prod_j^n z_j \cdot x_0) \theta(Q^2 - q_{\perp,n}^2) \quad (20)$$

We note that in this result most of the z -values are close to 1. We also note that, due to transverse momentum conservation and the ordering in eq. (16), the transverse momentum of the (quasi)real emissions, $q_{\perp,i}$, are approximately equal to the transverse momentum of the virtual links, which in fig. 8a are denoted $k_{\perp,i}$. Thus the variables $q_{\perp,i}$ in eq. (20) can to the given accuracy be replaced by the link variables $k_{\perp,i}$.

It is also possible to include the effects of the spin of the quarks by the exchange

$$\frac{1}{1-z} \rightarrow \frac{\frac{1}{2}(1+z^2)}{1-z} \quad (21)$$

Here the numerator corresponds to (half) the factor $(x_1^2 + x_2^2)$ in eq. (3), and does not change the behaviour near the dominating singularities at $z_i = 1$.

Taking the derivative of eq. (20) with respect to $\ln Q^2$ gives the following differential-integral equation (the DGLAP evolution equation):

$$\frac{\partial F(x, Q^2)}{\partial \ln Q^2} = \frac{4\alpha_s}{3\pi} \int dz dx' \hat{P}(z) F(x', Q^2) \delta(x - zx'). \quad (22)$$

It has here been possible to take the limit $\epsilon \rightarrow 0$, and thus remove the dependence on the cutoff. The ‘‘splitting function’’ P in eq. (21) is then

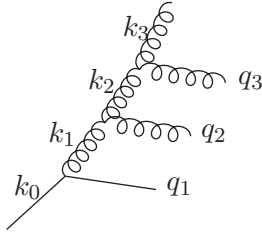


Fig. 9. A gluon ladder starting from a quark k_0 . The quasireal emissions have momenta q_i , while the virtual links are denoted k_i .

replaced by \hat{P} :

$$P = \frac{\frac{1}{2}(1+z^2)}{1-z} \rightarrow \hat{P} = \frac{\frac{1}{2}(1+z^2)}{(1-z)_+} + \frac{3}{2}\delta(1-z), \quad (23)$$

where the definition of the “+ prescription” is given by

$$\int \frac{dz}{(1-z)_+} \cdot f(z) \equiv \int dz \frac{f(z) - f(1)}{(1-z)} \quad (24)$$

for an arbitrary function $f(z)$. We note in particular that this definition implies that

$$\int \hat{P}(z) dz = 0, \quad (25)$$

which guarantees that the number of quarks is conserved.

4.4. Exclusive final states

We want to emphasise that eq. (22) only describes the probability for an interaction, that is the total photon-proton cross section expressed in terms of the structure function F_2 . To find the properties of exclusive final states it is necessary to add final state radiation within angular ordered regions, as indicated in fig. 8b. Just as the final state emission in e^+e^- -annihilation, these emissions do not affect the total cross section, and should therefore also be associated with appropriate Sudakov form factors.

4.5. Gluon rungs and small x

Also gluons can emit gluon radiation. Study the emission of gluon q_2 in fig. 9. With the notation in this figure the *eikonal current* corresponding to the first term in eq. (12) gives $g(k_1 + k_2)\epsilon_{q_2} (\epsilon_{k_1}\epsilon_{k_2})$. This term gives

a contribution similar to that for emission from a quark in eqs. (17, 18). Including now only the term singular at $z = 1$ we get

$$\frac{3\alpha_s}{\pi} \frac{dz_i}{1-z_i} \frac{dq_{\perp,i}^2}{q_{\perp,i}^2} \theta(q_{\perp,i} - q_{\perp,i-1}) \cdot S. \quad (26)$$

The spin factor $\epsilon_{k_1} \epsilon_{k_2}$ implies that the gluon spin is conserved along the vertical line in the ladder in fig. 9. We also note that, just as for quark emission, the pole at $z = 1$ implies that z -values close to 1 dominate. Thus gluon k_2 can be regarded as identical to the recoiling parent k_1 ; it inherits both the spin and most of the energy, while the gluon q_2 has to be regarded as a newborn soft gluon.

The *non-eikonal* contribution to the current is proportional to the remaining terms in eq. (12), $-(k_1 + q_2)\epsilon_{k_2}(\epsilon_{k_1}\epsilon_{q_2}) - (q_2 - k_2)\epsilon_{k_1}(\epsilon_{k_2}\epsilon_{q_2})$. Here the first term dominates (for a conventional gauge choice), and gives a contribution $\sim dz_i/z_i$:

$$\frac{3\alpha_s}{\pi} \frac{dz_i}{z_i} \frac{dq_{\perp,i}^2}{q_{\perp,i}^2} \theta(q_{\perp,i} - q_{\perp,i-1}). \quad (27)$$

Thus the “soft” gluon goes up the ladder, and it is the (quasireal) gluon q_2 , which takes over both the spin and most of the energy of the parent k_1 . The soft daughter does not replace the mother, and therefore there is *no Sudakov form factor* in leading order.

We note that soft gluon links can also be emitted from *quark* legs, as also indicated in fig. 9. The probability for this process has a different colour factor, and is proportional to

$$\frac{4\alpha_s}{3\pi} \frac{dz}{z} \frac{dq_{\perp}^2}{q_{\perp}^2}, \quad (28)$$

and also in this contribution there is no Sudakov form factor to leading order.

For gluonic chains the sum of the expressions in eqs. (26) and (27) replace the corresponding factor in eq. (20). The non-eikonal terms in eq. (27) give the dominant contributions for small z -values, and therefore also for small $x = (\prod z_i) x_0$. Thus gluon ladders are most important for the growth of the structure functions for small x , and to leading order in $\ln 1/x$ and $\ln Q^2$ the gluon density can be written

$$G(x, Q^2) \sim \sum_n \prod_i^n \left\{ \int \frac{4\alpha_s}{3\pi} \frac{dz_i}{z_i} \frac{dq_{\perp,i}^2}{q_{\perp,i}^2} \theta(q_{\perp,i} - q_{\perp,i-1}) \right\} \delta(x - \prod_j^n z_j \cdot x_0) \theta(Q^2 - q_{\perp,n}^2) \quad (29)$$

The gluon ladder may start from an initial quark with the coupling in eq. (28), and in DIS it must also have a quark link at the end, as the photon only couples to the electrically charged quarks. It is, however, the properties of the dominating gluonic ladder, which determines the asymptotic growth rate for small x .

4.6. Double Leading Log approximation

Assume that both Q^2 and $1/x$ are very large. We introduce the notation

$$x_i = \frac{k_i}{p_{\text{proton}}} = \prod_j^i z_j \quad (30)$$

$$\bar{\alpha} \equiv \frac{3\alpha_s}{\pi} \quad (31)$$

$$\kappa_i \equiv \ln(q_{\perp,i}^2/\Lambda^2) \quad (32)$$

$$l_i \equiv \ln(1/x_i) \quad (33)$$

For a fixed coupling $\bar{\alpha}$, we then find from eq. (29)

$$\begin{aligned} G &\sim \sum_n \left\{ \prod_i^n \int^{\ln Q^2} \bar{\alpha} d\kappa_i \theta(\kappa_i - \kappa_{i-1}) \cdot \prod_i^n \int^{\ln 1/x} dl_i \theta(l_i - l_{i-1}) \right\} = \\ &= \sum_n \bar{\alpha}^n \cdot \frac{(\ln Q^2)^n}{n!} \cdot \frac{(\ln 1/x)^n}{n!} = \\ &= I_0(2\sqrt{\bar{\alpha} \ln Q^2 \ln 1/x}) \sim \exp\left(2\sqrt{\bar{\alpha} \ln Q^2 \ln 1/x}\right), \end{aligned} \quad (34)$$

where I_0 is a modified Bessel function. This result corresponds to the Double Leading Log (DLL) approximation.

For a running α_s we define the parameter α_0 by the relation

$$\bar{\alpha} \equiv \frac{\alpha_0}{\ln(q_{\perp}^2/\Lambda^2)}. \quad (35)$$

We then have instead of $dq_{\perp,i}^2/q_{\perp,i}^2 = d\kappa_i$ a factor $d\kappa_i/\kappa_i = d\ln \kappa_i$, which gives the result

$$G \sim \exp\left(2\sqrt{\alpha_0 \cdot \ln \ln Q^2 \cdot \ln 1/x}\right). \quad (36)$$

5. Small x , the BFKL region

5.1. Non-ordered ladders

Now assume that Q^2 is not large, while x is still kept small. In this case the q_{\perp} -ordered phase space is small. Therefore q_{\perp} -non-ordered contributions are important, even if they are suppressed.

We mentioned after eq. (20) that for a q_{\perp} -ordered chain the transverse momentum of the (quasi)real emissions, $q_{\perp,i}$, are approximately equal to the transverse momentum of the virtual links, denoted $k_{\perp,i}$ in figs. 8 and 9. Therefore the variables $q_{\perp,i}$ in eqs. (20) and (29) could be replaced by the link variables $k_{\perp,i}$. This is no longer the case for non-ordered chains. Transverse momentum conservation implies that $\mathbf{q}_{\perp,i} = \mathbf{k}_{\perp,i-1} - \mathbf{k}_{\perp,i}$, and therefore we have, provided $\mathbf{k}_{\perp,i-1}$ and $\mathbf{k}_{\perp,i}$ are not approximately equal,

$$q_{\perp,i}^2 \approx \max(k_{\perp,i}^2, k_{\perp,i-1}^2). \quad (37)$$

Emissions for which $\mathbf{k}_{\perp,i-1} \approx \mathbf{k}_{\perp,i}$ will be discussed in subsection 5.5. They give no contribution to the structure functions, and can be treated as final state radiation. For other emissions eq. (37) implies that if *e.g.* $k_{\perp,i}$ is larger than the neighbouring links ($k_{\perp,i-1}$ and $k_{\perp,i+1}$), then $q_{\perp,i} \approx q_{\perp,i+1} \approx k_{\perp,i}$. If on the other hand $k_{\perp,i}$ is smaller than its neighbours, then its value is not close to any of the transverse momenta q_{\perp} . Thus the quasi-real momenta $q_{\perp,i}$ are approximately determined by the virtual links $k_{\perp,i}$, but the reverse is not true (without the knowledge of the azimuthal angles of all the vectors $\mathbf{q}_{\perp,i}$). To specify the chain we therefore have to specify the link variables $k_{\perp,i}$, and the distinction between $q_{\perp,i}$ and $k_{\perp,i}$ is essential.

Classical bremsstrahlung due to a short impulse during a time $\Delta t \sim 1/Q$ contains the factor

$$\sim \left| \int_0^{1/Q} dt e^{i\omega t} \right|^2 = \left| \frac{1}{\omega} (e^{i\omega/Q} - 1) \right|^2 = \begin{cases} \frac{1}{Q^2}, & \text{for } \omega \ll Q \\ \sim \frac{1}{\omega^2}, & \text{for } \omega \gg Q \end{cases} \quad (38)$$

Thus for $\omega \gg Q$ there is a relative suppression by a factor Q^2/ω^2 . In a relativistic calculation we should make the replacement $\omega \rightarrow q_{\perp}$. We then find that for $q_{\perp}^2 > Q^2$ the emission is not totally excluded; it is only reduced by a suppression factor Q^2/q_{\perp}^2 .

Assume that we have an ordered chain up to the last link with $k_{\perp,n}^2 \approx q_{\perp,n}^2$, which can be smaller or larger than Q^2 . We then find for these two cases:

- $k_{\perp,n}^2 < Q^2$.

In this ordered case we have $Q^2 > q_{\perp,n}^2 \approx k_{\perp,n}^2 > k_{\perp,n-1}^2$, and no extra suppression. According to eqs. (20) and (29) the contribution to the structure function from these chains contain a factor $1/q_{\perp,n}^2$. Therefore we have

$$\sigma \sim \frac{1}{Q^2} \cdot F \sim \frac{1}{Q^2 q_{\perp,n}^2}. \quad (39)$$

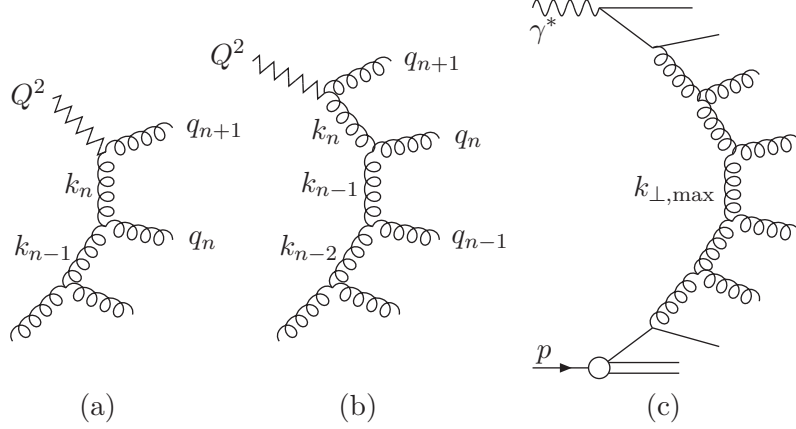


Fig. 10. (a) A situation where $k_{\perp,n}^2$ is larger than the virtuality Q^2 of the probe can be interpreted as a boson-gluon-fusion event, *i.e.* a hard subcollision between the probe and gluon k_{n-1} . (b) If $k_{\perp,n-1}^2$ is the largest virtuality, we have a hard subcollision between gluons k_{n-2} and k_n . (c) When the gluon with the largest transverse momentum is located in the middle of the chain, it corresponds to a hard subcollision between a proton and a resolved photon.

- $k_{\perp,n}^2 > Q^2$.

This implies $Q^2 < q_{\perp,n}^2 \approx k_{\perp,n}^2 > k_{\perp,n-1}^2$, and in this situation there is a suppression factor $Q^2/q_{\perp,n}^2$. Thus we have

$$\sigma \sim \frac{1}{Q^2} \cdot \frac{1}{q_{\perp,n}^2} \cdot \frac{Q^2}{q_{\perp,n}^2} \sim \frac{1}{k_{\perp,n}^4}. \quad (40)$$

In the latter case we see that the process can be interpreted as a hard subcollision between the probe and the gluon k_{n-1} , *cf.* fig. 10a. (Instead of a photon we imagine here a hypothetical colour neutral probe, which can interact directly with gluons.) We recognize the expected result from a hard scattering with momentum exchange $t = -k_{\perp,n}^2$, which is then the largest virtuality in the process.

Assume now that we have a situation where the last but one gluon link, k_{n-1} , has the largest transverse momentum, which implies:

- $Q^2 < k_{\perp,n}^2 < q_{\perp,n-1}^2 \approx k_{\perp,n-1}^2 \approx q_{\perp,n-2}^2 > k_{\perp,n-2}^2$.

We expect here a suppression factor $Q^2/q_{\perp,n-1}^2 \approx Q^2/k_{\perp,n-1}^2$. This factor can be written as a product of two separate factors, one for each step

downwards in k_{\perp} :

$$\frac{Q^2}{k_{\perp,n-1}^2} = \frac{k_{\perp,n}^2}{k_{\perp,n-1}^2} \cdot \frac{Q^2}{k_{\perp,n}^2} \quad (41)$$

As illustrated in fig. 10b, this process can be interpreted as a hard sub-collision between the links k_n (now coming from above) and k_{n-2} , with momentum transfer $k_{\perp,n-1}^2$. The outgoing gluons have approximately equal but opposite transverse momenta, $q_{\perp,n-1}$ and $q_{\perp,n}$, and the cross section satisfies the expected relation $\sigma \sim 1/k_{\perp,n-1}^4$.

These results can be generalized to the situation in fig. 10c, where k_{\perp} increases continuously from the proton, up to a maximum value $k_{\perp,\max}$, and then decreases in k_{\perp} down to the virtuality, Q^2 , of the photon. This process has a weight with a factor $1/k_{\perp,i}^2$ for every links except k_{\max} , which instead gives a factor $1/k_{\perp,\max}^4$. We note here that, although upwards and downwards steps are treated differently, the final result is *symmetric* in the sense that we could equally well have started the chain from the photon end, and proceeded towards the proton. Therefore it is identical to the result obtained from a DGLAP evolution for both the proton in one end and a *resolved photon* in the other end, up to a central hard scattering, with momentum transfer $k_{\perp,\max}$.

With enough energy it is apparently also possible to have ladders in which the transverse momentum goes up and down with two or more local maxima. When expressed in the virtual links k_{\perp} , each step downwards corresponds to a suppression factor $k_{\perp,i}^2/k_{\perp,i-1}^2$. The net result is a factor $1/k_{\perp}^4$ for every local maximum k_{\perp} , but no k_{\perp} -power for links corresponding to a local minimum.

We formulated the result in terms of the link variables $k_{\perp,i}^2$, because these could be interpreted as independent variables. Transverse momentum conservation implies that the quantities $q_{\perp,i}$ are not independent, but constrained by the relation $q_{\perp,\max}^2 \approx q_{\perp,\max+1}^2$, and they do not fix the value of k_{\perp}^2 for a link which represents a local minimum. We note, however, that the weight for the chain corresponds exactly to the product $\prod_i^n q_{\perp,i}^{-2}$. The factor $q_{\perp,\max}^{-2} \cdot q_{\perp,\max+1}^{-2}$ gives the factor $1/k_{\perp,\max}^4$, and the k_{\perp} for a local minimum, which does not equal any q_{\perp} , does not appear in the weight.

We further note that, if the azimuthal angles are not averaged over, but properly accounted for, we have $d^2k_{\perp,i} = d^2q_{\perp,i}$. As a consequence we see that our result exactly corresponds to the ordered result in eq. (29), if we make the replacement

$$\frac{dq_{\perp,i}^2}{q_{\perp,i}^2} \rightarrow \frac{d^2q_{\perp,i}}{\pi q_{\perp,i}^2}, \quad (42)$$

omit the ordering θ -functions and instead include a factor

$\theta(q_{\perp,i} - \min(k_{\perp,i}, k_{\perp,i-1}))$. This factor excludes soft emissions for which $\mathbf{k}_{\perp,i} \approx \mathbf{k}_{\perp,i-1}$, as mentioned above and is further discussed in section 5.5. Thus the expression

$$G \sim \sum_n \prod_i^n \left\{ \int \frac{4\alpha_s}{3\pi} \frac{dz_i}{z_i} \frac{d^2 q_{\perp,i}}{\pi q_{\perp,i}^2} \theta(q_{\perp,i} - \min(k_{\perp,i}, k_{\perp,i-1})) \right\} \delta(x - \prod_j^n z_j \cdot x_0) \quad (43)$$

gives a proper description, both for large Q^2 and ordered chains, and for limited Q^2 when non-ordered chains are important. To get the non-integrated distribution function \mathcal{G} , we just have to add a factor $\delta(\mathbf{k}_{\perp,n} + \sum_j^n \mathbf{q}_{\perp,j})$, which follows from conservation of transverse momentum.

This result also demonstrates the symmetry discussed above. An important consequence of this symmetry is that the formalism also is suitable for describing hard subcollisions in hadronic collisions. This will be further discussed in section 6.

5.2. Effective phase space

With more than one local maximum in the k_{\perp} chain, we find for every step down from $k_{\perp,i-1}^2$ to $k_{\perp,i}^2$ a suppression factor $k_{\perp,i}^2/k_{\perp,i-1}^2$. Expressed in the logarithmic variable $\kappa = \ln k_{\perp}^2$, this corresponds to a factor $\exp[-(\kappa_{i-1} - \kappa_i)]$. This implies that *the effective range allowed for downward steps corresponds to approximately one unit in κ* . Consequently we find instead of the phase space limits in eq. (16), the following boundaries (replacing $q_{\perp,i}^2$ by $k_{\perp,i}^2$, which are the relevant variables for non-ordered chains)

$$\ln k_{\perp,i}^2 \gtrsim \ln k_{\perp,i-1}^2 - 1. \quad (44)$$

This modification changes the DLL result in eqs. (34) and (36) in a qualitative way, as described in the following subsections.

5.3. Fixed α_s

For a fixed α_s , and writing κ for $\ln Q^2$, we then find for the transverse momentum integrals in eq. (34) instead of

$$\int_0^{\kappa} \prod_i^n d\kappa_i \theta(\kappa_i - \kappa_{i-1}) = \frac{\kappa^n}{n!}, \quad (\kappa = \ln Q^2) \quad (45)$$

the following result

$$\int_0^{\kappa} \prod_i^n d\kappa_i \theta(\kappa_i - \kappa_{i-1} - 1) \approx \frac{(\kappa + n)^n}{n!} \quad (46)$$

When κ is very large we recover the DLL result in eq. (34), but for smaller values of κ we find instead using Sterling's formula

$$\kappa \text{ small} \Rightarrow \frac{(\kappa + n)^n}{n!} \sim \frac{n^n}{n!} \sim e^n \quad (47)$$

which implies

$$G \sim \sum_n \frac{[\bar{\alpha} e \ln(1/x)]^n}{n!} = e^{e \bar{\alpha} \ln(1/x)} = \frac{1}{x^\lambda} \quad (48)$$

with

$$\lambda = e \bar{\alpha} \approx 2.72 \bar{\alpha}. \quad (49)$$

To obtain the non-integrated distribution $\mathcal{G}(x, k_\perp^2)$, we add the factor $\delta(\mathbf{k}_\perp - \mathbf{k}_{\perp, n})$, but this does not modify the qualitative result, if κ now denotes $\ln k_\perp^2$.

The result in eq. (48) is relevant for $\ln k_\perp^2 < e \bar{\alpha} \ln(1/x)$. In this range the chain corresponds to a random walk in $\ln k_\perp^2$. Our result should be compared with the result from the leading order BFKL equation, which gives

$$\lambda = 4 \ln 2 \bar{\alpha} \approx 2.77 \bar{\alpha}. \quad (50)$$

We see that this simple semiclassical picture describes the essential features of BFKL evolution.

5.4. Running α_s

For a running α_s the steps in transverse momentum are determined by the factors

$$\alpha_0 \frac{d \ln k_{\perp, i}^2}{\ln k_{\perp, i}^2} = \alpha_0 d(\ln \ln k_{\perp, i}^2) \quad (51)$$

When k_\perp is large, one extra unit in $\ln k_\perp^2$ corresponds to a very small extra space in $\ln \ln k_\perp^2$. This implies that, once the chain has reached large k_\perp -values, it is very difficult to come down again. Therefore dominant chains will contain an initial part with low k_\perp and steps up and down, and a second (DGLAP-like) part with increasing k_\perp up to the final k_\perp - and x -values. As a consequence the structure functions can be well described by DGLAP evolution from adjusted input distributions $f_0(x, k_{\perp 0}^2)$, which grow for small values of x .

For further discussions of the results in this and the previous sections, see ref. [11].

5.5. Exclusive final states

As discussed above in connection with large- Q^2 phenomena, final state radiation must be added, in order to describe the properties of exclusive final states. The kinematic regions in which such emission should be allowed is in general dependent on the formalism used. The quasireal gluons, denoted q_i in figs. 8 and 9, are allowed to emit final state radiation in angular ordered regions, but besides within these regions further soft emissions may also be possible.

In all discussions of the results in the previous sections we studied chains in which at every vertex the emitted q_{\perp} approximately equals the larger of the adjoining k_{\perp} . We could also imagine the emission of a softer gluon, with $q_{\perp,i} \ll k_{\perp,i-1}$, which then implies $\mathbf{k}_{\perp,i} \approx \mathbf{k}_{\perp,i-1}$. From the discussion about formation time in section 2.2, such emissions should take place at a longer time scale, after formation of the interaction chain in figure 8a or 9. They should therefore not influence the reaction probability, *i.e.* the structure function, but only affect the properties of exclusive final states. Consequently they may be treated as final state radiation, and must be associated with appropriate Sudakov form factors. This is indeed the result obtained in a perturbative calculation, in which such emissions are compensated by virtual corrections, and in the BFKL formalism this effect is described by treating the link gluons as *Reggeized gluons*. Such final state radiation may be emitted both from gluon and quark links, and one example was indicated in fig. 8b.

These emissions are also treated as final state radiation in the *Linked Dipole Chain* (LDC) model for DIS [4], which will be further discussed in the next section. We note, however, that the separation between initial and final state radiation is not defined by nature, but depends on the formalism used. This separation is defined in a different way in the CCFM formalism [3], in which some emissions, for which $\mathbf{k}_{\perp,i} \approx \mathbf{k}_{\perp,i-1}$, are treated as initial state radiation. This implies that in this formalism the initial chains generally contain a larger number of links, and that final state radiation is correspondingly allowed in a more restricted kinematic region. A consequence is that a larger set of chains contribute in the calculation of \mathcal{G} , with each chain given a smaller weight. This reduction is represented by a “non-eikonal form factor”, in such a way that the BFKL result is reproduced to leading log accuracy. For further discussions of this difference between the formalisms see refs. [4] and [12].

6. Linked Dipole Chain model

6.1. LDC for DIS

The Linked Dipole Chain (LDC) model [4] is a reformulation and generalization of the CCFM model. Thus it is based on perturbative QCD calculations, and can be regarded as a formal quantum mechanical derivation of the semiclassical results presented above.

The LDC model is based on the observation that the dominant features of the parton evolution is determined by a subset of emitted gluons, which are ordered in both positive and negative light-cone components, and also satisfy the relation

$$q_{\perp,i} > \min(k_{\perp,i}, k_{\perp,i-1}). \quad (52)$$

In LDC this subset of “*primary*” gluons forms a chain of initial state radiation, and all other emissions are treated as final state radiation (including those emissions, which would be emitted from a virtual link k_i , rather than from a quasireal emission q_i , as discussed in section 5.5). In ref. [4] it is shown that adding the contributions from all different CCFM-chains with the same primary gluons, with their non-eikonal form factors, gives the following simple result:

$$\mathcal{G} \approx \sum_n \prod_i^n \iint \bar{\alpha} \frac{dz_i}{z_i} \frac{d^2 q_{\perp,i}}{\pi q_{\perp,i}^2} \theta(q_{\perp,i} - \min(k_{\perp,i}, k_{\perp,i-1})) \delta(x - \prod z_j) \quad (53)$$

where the link momenta $\mathbf{k}_{\perp,i} = \sum_j^i \mathbf{q}_{\perp,j}$ are determined by transverse momentum conservation. This implies that

$$q_{\perp,i}^2 \approx \max(k_{\perp,i}^2, k_{\perp,i-1}^2) \quad (54)$$

From this relation we find for a step up or down in k_{\perp} :

- Step up in k_{\perp} : $k_{\perp,i} > k_{\perp,i-1} \Rightarrow q_{\perp,i} \approx k_{\perp,i}$, which implies

$$\frac{d^2 q_{\perp,i}}{q_{\perp,i}^2} \approx \frac{d^2 k_{\perp,i}}{k_{\perp,i}^2} \quad (55)$$

- Step down in k_{\perp} : $k_{\perp,i} < k_{\perp,i-1} \Rightarrow q_{\perp,i} \approx k_{\perp,i-1}$, which implies

$$\frac{d^2 q_{\perp,i}}{q_{\perp,i}^2} \approx \frac{d^2 k_{\perp,i}}{k_{\perp,i-1}^2} = \frac{d^2 k_{\perp,i}}{k_{\perp,i}^2} \cdot \frac{k_{\perp,i}^2}{k_{\perp,i-1}^2} \quad (56)$$

We here recognize the suppression factor $k_{\perp,i}^2/k_{\perp,i-1}^2$ in eq. (41), associated with a step down in k_{\perp} .

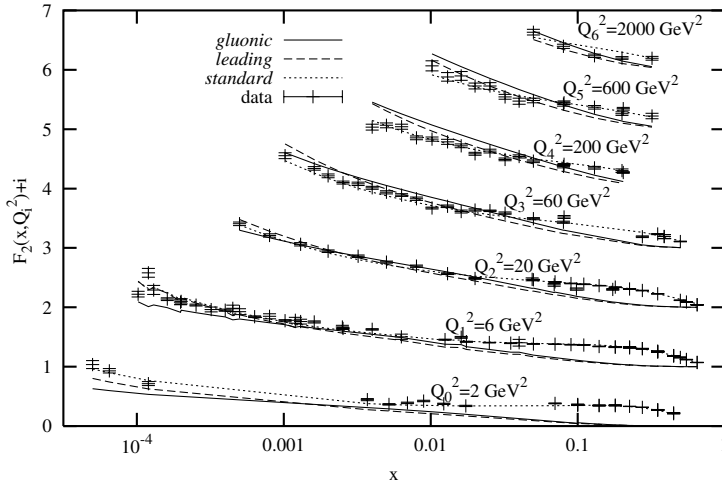


Fig. 11. The description of F_2 data as a function of x for different Q^2 . To separate the results, what is shown is $F_2 + i$ for Q_i^2 . Both small and large x data from H1, ZEUS, NMC and E665 are included [16]. The favoured fit is the one called standard and denoted by dotted lines. In this fit both gluon and quark links are included. For a detailed description of the fits, see ref. [15].

Non-leading contributions from $1/(1-z)$ -poles and quark links are added with Sudakov form factors. In this formalism it is natural to include a running coupling

$$\alpha_s(q_{\perp,i}^2) = \alpha_s(\max(k_{\perp,i}^2, k_{\perp,i-1}^2)) \quad (57)$$

Note, however, that this increase of α_s for soft emissions necessarily implies that a cutoff is needed for soft k_{\perp} [13]. This dividing line between the perturbative and the nonperturbative regimes has to be adjusted by fits to experimental data.

A Monte Carlo implementation, called LDCMC, is developed by H. Kharraziha and L. Lönnblad [14]. This program does reproduce a large set of experimental data. Fig. 11 shows a fit to F_2 [15], compared with data from HERA and fixed target experiments. The corresponding gluon distribution is shown in fig. 12, and we note that this result shows good agreement with the results from the CTEQ [17] and MRST [18] fits. (Note that the LDC result is fitted to DIS data only, while the CTEQ and MRST fits include data from hadronic collisions.) As mentioned above, the LDC model is a generalization of the CCFM model, which is implemented in the event generator CASCADE [19]. Both LDCMC and CASCADE reproduce the main features of

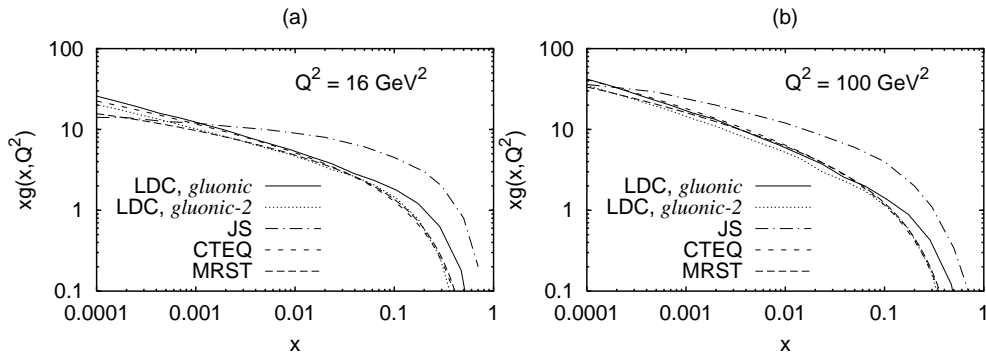


Fig. 12. The LDC integrated gluon distribution function for two different fits (called “gluonic” and “gluonic-2”), compared to the corresponding results from CASCADE denoted JS (dash-dotted curve), CTEQ (short-dashed curve) and MRST (long-dashed curve), for (a) $Q^2 = 16 \text{ GeV}^2$ and (b) $Q^2 = 100 \text{ GeV}^2$.

the final state properties [20]. A problem is, however, that both models are able to reproduce the forward jet cross section only if the non-singular terms in the splitting functions are omitted [20]. We do not know whether these terms are compensated by some dynamical mechanism, or if the modelling of the proton fragmentation has to be improved.

6.2. Hadronic collisions

The LDC formalism can be applied also to hadron-hadron collisions [21, 22]. In hadronic collisions *multiple interactions* are needed to describe associated multiplicity and transverse energy in events with high p_{\perp} jets. Such multiple interactions can originate either from two hard subcollisions in a single parton chain, *or* from more than one chain in a single event.

The LDC formalism is very suitable for describing such events. A potential problem arises because good fits to DIS data can be obtained for different values for the low k_{\perp} cutoff, provided that the soft input structure function is adjusted accordingly. This is important because the number of hard chains depends on this soft cutoff. If the cutoff is increased a more singular input gluon distribution is needed in the fit to F_2 . These soft input gluons, present at scale Q_0^2 , may also form “soft chains” between the two colliding protons. These soft chains then have no emitted gluons with q_{\perp} above Q_0 , but they do produce hadrons with low p_{\perp} . From the fits to DIS data we then find that the reduction in the number of hard chains is just compensated by an increase in the number of soft chains, as is illustrated in fig 13. As a result we see that, in this formalism, the (average) total

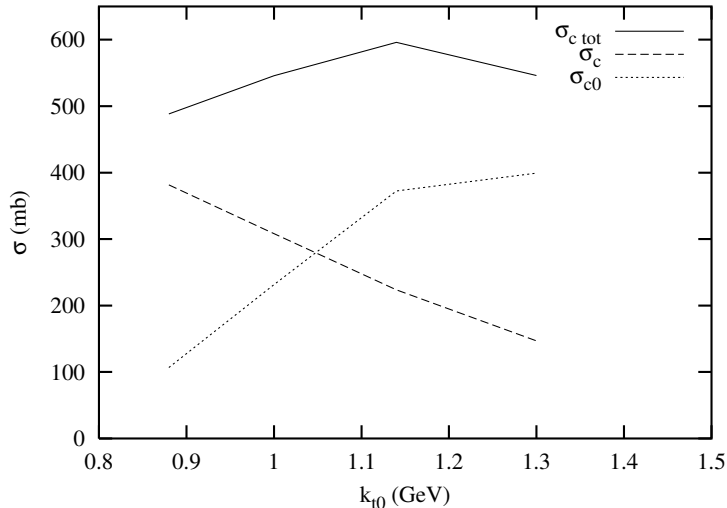


Fig. 13. The cross section per chain in the LDC model as a function of the cutoff, $k_{\perp 0}^2$. The dashed line is the cross section for chains with at least one emission above the cutoff, the dotted line is for soft chains without emissions above the cutoff, and the full line is the sum of the two. Note that the input parton densities have been re-fitted for each value of $k_{\perp 0}$.

number of chains in a pp collision can be fixed by fits to DIS data. This result apparently implies a very strong connection between DIS and hadronic collisions [22].

This formalism should also be applicable in studies of effects of unitarisation and saturation. Separate branches of a chain can interact with a colliding hadron, or different chains can join each other, and these possibilities are presently under study. Also applications to diffractive collisions are of interest.

7. Conclusions

We have seen that the behaviour of DIS in the DGLAP and BFKL domains can be understood in a semiclassical intuitive picture. A more quantitative description is offered by the LDC formalism, which smoothly interpolates between these two kinematical regions.

The formalism also offers a link between DIS and hadronic collisions. Within the formalism fits to data on F_2 in DIS can be used to predict the number of chains and hard subcollisions in a high energy proton-proton collision.

Further work on multiple interaction and saturation is in progress, as well as studies of diffractive scattering.

8. Acknowledgement

I want to thank my collaborators Leif Lönnblad and Gabriela Miu.

REFERENCES

- [1] E. Bloom *et al.* *Phys. Rev. Lett.* **23** (1969) 930.
- [2] E. A. Kuraev, L. N. Lipatov, and V. S. Fadin *Sov. Phys. JETP* **45** (1977) 199, I. I. Balitsky and L. N. Lipatov *Sov. J. Nucl. Phys.* **28** (1978) 822.
- [3] M. Ciafaloni *Nucl. Phys.* **B296** (1988) 49, S. Catani, F. Fiorani, and G. Marchesini *Phys. Lett.* **B234** (1990) 339.
- [4] B. Andersson, G. Gustafson and J. Samuelsson *Nucl. Phys.* **B467** (1996) 443, B. Andersson, G. Gustafson and H. Kharraziha *Phys. Rev.* **D57** (1998) 5543, hep-ph/9711403.
- [5] A.H. Mueller *Phys. Lett.* **B104** (1981) 161, B.I. Ermolaev and V.S. Fadin *JETP Lett.* **33** (1981) 269, A. Bassetto, M. Ciafaloni, G. Marchesini, and A.H. Mueller *Nucl. Phys.* **B207** (1982) 189, G. Marchesini and B. Webber *Nucl. Phys.* **B238** (1984) 1.
- [6] G. Gustafson *Phys. Lett.* **B175** (1986) 453.
- [7] G. Gustafson and U. Pettersson *Nucl. Phys.* **B306** (1988) 746.
- [8] L. Lönnblad *Comput. Phys. Commun.* **71** (1992) 15.
- [9] K. Hamacher and M. Weierstall, “The Next Round of Hadronic Generator Tuning Heavily Based on Identified Particle Data”, hep-ex/9511011.
- [10] B. Andersson, G. Gustafson, G. Ingelman, and T. Sjöstrand *Phys. Rept.* **97** (1983) 31.
- [11] G. Gustafson and G. Miu *Eur. Phys. J.* **C23** (2002) 267, hep-ph/0110143
- [12] G. Salam *JHEP* **9903** (1999) 009.
- [13] E.M. Levin and M.G. Ryskin *Phys. Rept.* **189** (1990) 267, J. Bartels and H. Lotter *Phys. Lett.* **B309** (1993) 400, J.R. Forshaw, P.N. Harriman, and P.J. Sutton *Nucl. Phys.* **B146** (1994) 739.
- [14] H. Kharraziha and L. Lönnblad *JHEP* **03** (1998) 006, hep-ph/9709424.
- [15] G. Gustafson, L. Lönnblad, and G. Miu *JHEP* 0209 (2002) 005, hep-ph/0206195.
- [16] **H1** Collaboration, S. Aid *et al.* *Nucl. Phys.* **B470** (1996) 3, hep-ph/9603004, **ZEUS** Collaboration, M. Derrick *et al.* *Z. Phys.* **C72** (1996) 399, hep-ph/9607002, **New Muon** Collaboration, M. Arneodo *et al.* *Phys. Lett.* **B364** (1995) 107, hep-ph/9509406, **E665** Collaboration, M.R. Adams *et al.* *Phys. Rev.* **D54** (199) 3006.

- [17] **CTEQ** Collaboration, H. L. Lai *et al.* *Eur. Phys. J.* **C12** (2000) 375, hep-ph/9903282.
- [18] A. D. Martin, R. G. Roberts, W. J. Stirling, and R. S. Thorne *Eur. Phys. J.* **C23** (2002) 73, hep-ph/0110215.
- [19] H. Jung *Comput. Phys. Commun.* **143** (2002) 100, hep-ph/0109102,
H. Jung and G.P. Salam *Eur. Phys. J.* **C19** (2001) 351, hep-ph/0012143.
- [20] **Small x** Collaboration, B. Andersson *et al.* hep-ph/0204115.
- [21] G. Gustafson and G. Miu *Phys. Rev.* **D63** (2001) 034004, hep-ph/0002278.
- [22] G. Gustafson, L. Lönnblad, and G. Miu *Phys.Rev.* **D67** (2003) 034020, hep-ph/0209186.